Journal of Applied Polymer Science

Mass transfer kinetics and diffusion coefficient estimation of bioinsecticide terpene ketones in LDPE films obtained by supercritical CO_2-assisted impregnation

María Laura Goñi,[1,2] **Nicolás Alberto Gañán**,[1,2] **Raquel Evangelina Martini**,[1,2] **Miriam Cristina Strumia**[1]

[1]IPQA, Universidad Nacional de Córdoba, CONICET, Córdoba X5016GCA, Argentina

[2]ICTA—Instituto de Ciencia y Tecnología de los Alimentos, FCEFYN, Universidad Nacional de Córdoba, Córdoba X5016GCA, Argentina

Correspondence to: M. L. Goñi (E-mail: lauragoni@gmail.com)

ABSTRACT: Release kinetics of thymoquinone and *R*-(+)-pulegone impregnated in low-density polyethylene (LDPE) films into air and the effect of supercritical CO_2-assisted impregnation process on the diffusional properties of these films were investigated. The incorporation of both ketones into LDPE films was performed under different conditions (pressure, depressurization rate, time, and initial ketone mole fraction). Release experiments were performed under controlled laboratory conditions (24 °C, 60% relative humidity), and the total release profile was determined gravimetrically, while the individual release of each ketone was quantified by Fourier transformed infrared. The experimental data were used to fit a mass transfer model based on the second Fick's law for unsteady-state diffusion, and the diffusion coefficients of both ketones in LDPE were estimated, ranging from 2.35×10^{-13} to 5.53×10^{-13} $m^2\ s^{-1}$ (thymoquinone) and from 1.24×10^{-13} to 4.52×10^{-13} $m^2\ s^{-1}$ (pulegone). Finally, analysis of variance testing indicated that impregnation pressure and depressurization rate (and their combination) have significant effects on the diffusion coefficient values. © 2017 Wiley Periodicals, Inc. J. Appl. Polym. Sci. **2017**, *134*, 45558.

KEYWORDS: films; packaging; polyolefins; synthesis and processing techniques

Received 24 April 2017; accepted 14 July 2017

DOI: 10.1002/app.45558

INTRODUCTION

Supercritical carbon dioxide ($scCO_2$)-assisted impregnation has been proposed and studied by many authors as an attractive technique for the incorporation of active compounds into polymeric matrices, with potential applications ranging from drug delivery systems to active food packaging.[1–5] Among the main advantages of this technology, we can mention: (a) CO_2 is a gas at ambient pressure, therefore solvent-free products are obtained by simple decompression; (b) it can operate at low temperature conditions, thus preserving thermolabile compounds (the critical temperature of CO_2 is 31 °C); (c) $scCO_2$ is readily soluble in many polymers, promoting their swelling and favoring the internal diffusion of solutes, achieving high penetration degrees within short time periods.[6]

In fact, the efficiency of the impregnation process relies on the sorption of $scCO_2$ by the polymeric matrix. CO_2 molecules diffuse among the polymer chains, increasing the system free volume and acting as a "lubricant" by enhancing their mobility and the diffusion of solute molecules.[1] This transitory plasticizing effect is reversed during depressurization, as CO_2 is desorbed from the polymer and the free volume decreases. As solute molecules generally diffuse at a lower rate than CO_2, a significant amount can be retained into the polymer after depressurization. The strong specific interactions occurring between CO_2 and the polymer functional groups (such as acrylates) enhance sorption and polymer swelling,[7] while the interactions between solute molecules and polymer chains enhance impregnation yield.[8] The physicochemical description of the $scCO_2$ sorption and impregnation process in different types of polymers (crystalline and amorphous, glassy and rubbery) has been extensively covered and reviewed by many authors.[3,9–13]

In general, the incorporation of low-molecular-weight compounds into polymeric matrices has a plasticizing effect, with a consequent depression of the glass transition temperature.[14] Furthermore, the high pressure treatment itself (usually above 8–10 MPa) followed by depressurization, involved in $scCO_2$ impregnation processes, may also affect the polymer structure permanently, with changes in morphology, mechanical, and diffusional properties.[15] In other words, the transitory

modification of polymer properties under high pressure may not be completely reversible. A dramatic example of this behavior is the formation of foam-like materials by rapid depressurization of amorphous polymers such as poly(methyl methacrylate),[15] with very high CO_2 sorption capacity. In other cases, when CO_2 sorption is low or when the pressurization–depressurization cycle is less severe, it is expectable that the polymer morphological properties may be less affected.

The assessment of these changes in the polymer morphology, which can in turn affect the diffusional properties, is a key aspect for the technological application of the impregnated material.[5] In this article, we attempt to evaluate this phenomenon in a practical case.

In a previous work,[16] the authors have studied the $scCO_2$-assisted impregnation of a commercial semi-crystalline low density polyethylene (LDPE) film with an equimolar mixture of two natural terpene ketones [*R*-(+)-pulegone and thymoquinone]. These ketones have been previously investigated as potential bioinsecticides against the maize weevil, *Sitophilus zeamais* Motschulsky,[17–19] a common primary pest of stored grains. Using a fractional factorial experimental design, the effect of different operation parameters on the impregnation efficiency was evaluated. These parameters were as follows: impregnation pressure (10 and 15 MPa), depressurization rate (0.5 and 2 MPa min^{-1}), contact time (2 and 4 h), and initial ketone concentration in the fluid phase (0.0017 and 0.0025, mole fraction). The impregnated material, with total ketone content ranging from 2% to 6% (wt/wt), proved to be effective in creating a lethal fumigant atmosphere against *S. zeamais* adults in confined environments, suggesting its possible application as delivery device for the protection of grains during storage and/or transport.[16] For example, it could be envisaged as a part of multilayer silo bags in order to avoid the proliferation of weevils into the bag if it is damaged. Other strategies have been attempted in order to increase the amount of active compound loaded into the polymer films as well as its retention such as the incorporation of nanoparticles with sorption properties into the films prior impregnation.[20]

The design and modeling of this kind of materials—for example, for predicting their performance along time and estimating their life time—requires some knowledge of the diffusional properties, as the active substance release kinetics is mainly controlled by diffusion in the polymer. This is also necessary if the polymer will be in contact with gaseous or liquid environments, absorbing compounds which can affect its properties or affect the organoleptic profile of the product (e.g., the absorption of aroma compounds or "scalping" in fruit juices).[21,22]

There are different techniques for determining the diffusion coefficient of a solute through a polymeric film or membrane, namely: (i) sorption/desorption kinetic studies; (ii) permeation methods; and (iii) concentration–distance curves.[23,24] In sorption kinetic studies, the polymer is put in contact with the pure solute in liquid or gaseous form, or with a solution of it, and the amount of solute absorbed is quantified as a function of time. In the case of desorption from a loaded polymer, it can be performed in air (if the solute is volatile) or in a proper liquid extraction solvent, and the amount of solute released is measured. In permeation methods, the flux of solute passing through the polymeric film is measured, after reaching steady-state conditions. Finally, in concentration–distance methods the solute concentration profile inside the polymeric matrix is measured as a function of time. In all these methods, the solute diffusion coefficient value is determined by fitting the experimental data to a proper mass transfer model. Besides, molecular simulation tools have also been proposed for the estimation of diffusional properties in polymers based on theoretical grounds.[25]

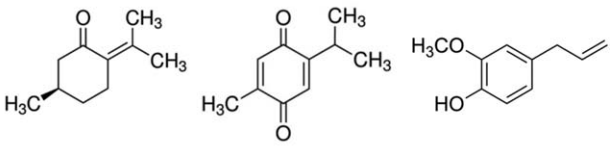

Figure 1. Chemical structure of: (a) *R*-(+)-pulegone, (b) thymoquinone, (c) eugenol.

In this work, the desorption kinetics of thymoquinone and *R*-(+)-pulegone from $scCO_2$-impregnated LDPE films into air is determined by a combination of gravimetric measurements (for total release) and Fourier transformed infrared (FTIR) spectrometry (for individual compounds). From this data, the diffusion coefficient of both ketones in the films are estimated by applying a mass transfer model based on an analytical solution of second Fick's law. The obtained values are statistically analyzed and explained in terms of the impregnation process conditions and its effects on the polymer morphological properties.

EXPERIMENTAL

Materials

R-(+)-pulegone (≥97%; MW: 152.2 g mol^{-1}; bp: 224 °C), thymoquinone (≥99%; MW: 164.2 g mol^{-1}; m.p.: 45 °C), and eugenol (≥99%; MW: 164.2 g mol^{-1}; b.p.: 254 °C) were purchased from Sigma-Aldrich (Steinheim, Germany). Their chemical structure is shown in Figure 1. Commercial LDPE film (M_w: 229,300 g mol^{-1}; M_n: 22,500 g mol^{-1}, melt flow index (MFI) : 0.6 g/10 min at 190 °C/2.16 kg; density: 921 kg m^{-3}; thickness: 130 ± 20 μm) was provided by Dow-Polisur (Bahía Blanca, Argentina). Paraffin oil (medicinal grade; density: 870 kg m^{-3}; Sanitas S.A., Argentina) was used as solvent in the FTIR analysis calibration.

Experimental Procedure

Supercritical CO_2-Assisted Impregnation. The impregnation of the LDPE films has been described and analyzed in a previous paper,[16] as mentioned. Briefly, film samples were impregnated with an equimolar mixture of thymoquinone and *R*-(+)-pulegone using $scCO_2$ as solvent under different combinations of four process parameters at two levels, according to a 3/4 fractional factorial experimental design of 12 runs: (A) pressure (10 and 15 MPa); (B) depressurization rate (0.5 and 2 MPa min^{-1}); (C) contact time (2 and 4 h); (D) initial ketone concentration in the fluid phase (0.0017 and 0.0025, mole fraction). The temperature (45 °C) and agitation rate (900 rpm) were constant in all runs. The impregnation yield (i.e., the concentration of

ketones into the impregnated films) ranged between 2% and 6% (wt/wt). The film samples were stored in sealed vials, protected from light and refrigerated (4 °C) until analysis.

Release Kinetics. The total release kinetics of both ketones was determined gravimetrically by quantifying the weight loss of the impregnated films along time in a precision balance (±0.0001 g). Rectangular film samples of ~5 cm^2 were placed in Petri dishes in vertical position, in order to allow the release from both sides, and were weighed at different time intervals until reaching constant weight (within the error of the balance). The release process was conducted in a laboratory at ambient pressure and constant temperature (24 °C), with air ventilation and controlled relative humidity (~60%). Pure LDPE film was used as control sample in order to check possible variations due to water vapor adsorption or desorption. The thickness of each film sample was measured using a precision micrometer (0–25 mm × 0.01 mm, Wembley, China).

After each weight measurement, the film samples were immediately analyzed by FTIR spectrometry, in order to quantify the relative residual concentration of pulegone and thymoquinone in the films during the release process, which in turn allowed to calculate the corresponding released amounts by a mass balance. Combining both gravimetric and spectrometric data, cumulative release curves for each ketone were constructed. Absorbance spectra were obtained in an infrared imaging microscope (Nicolet iN10 Mx, Thermo Fisher Scientific, Waltham, MA) in transmission mode, with a resolution of 4 cm^{-1}, in a wavenumber range of 400–4000 cm^{-1} with 16 scans, at room temperature (24 °C). Based on the analysis of spectra of the pure ketones, original LDPE film, and impregnated film samples, reported in a previous work,[16] characteristic absorbance peaks were identified and their relative absorbance values were quantified after multipoint linear baseline correction. Measurements were performed at five different positions of each film, including points near the edges (upper and lower), and far from the edges ("center"), in order to check the homogeneity of ketones distribution. Background spectra were acquired before each test for air humidity and carbon dioxide correction. The ratio between the concentration of both ketones in the films was assessed by comparing the relative absorbance values of the characteristic peaks for each compound. For that purpose, a calibration curve was prepared using different ketone mixtures dissolved in paraffin oil (in order to obtain a molecular environment similar to LDPE)[26] with thymoquinone:pulegone mass ratios ranging from 25:75 to 75:25, as reported in a previous work.[16] The total ketone concentration in all the mixtures assayed was constant and equal to 5% (wt/wt), close to the initial concentration of ketones in the impregnated films. The relationship between the concentration ratio of thymoquinone and pulegone in this set of solutions and their relative absorbance was adjusted with a linear function, according to eq. (1).

$$\frac{A_{thym}}{A_{pul}} = a\left(\frac{C_{thym}}{C_{pul}}\right) + b \quad (1)$$

Where A_{thym} and A_{pul} are the absorbance values for the characteristic peaks of thymoquinone and pulegone, respectively, as well as C_{thym} and C_{pul} are their mass concentrations in the ketone mixtures. In this way, results are independent of the optical path length. The parameters a and b were determined by linear regression. The calibration curve was performed by duplicate, and each measurement was replicated four times.

Model Equations and Calculations. The diffusion coefficient values for each ketone (D_P and D_T for pulegone and thymoquinone, respectively) in each film sample were obtained by fitting a mathematical model, based on the second Fick's law for non-steady state diffusion [eq. (2)], to the corresponding experimental cumulative release curves:

$$\frac{\partial C}{\partial t} = D\frac{\partial^2 C}{\partial^2 x} \quad (2)$$

where C is the concentration of the diffusive species and D is its diffusion coefficient. This equation is subject to specific initial and boundary conditions depending on the geometry and characteristics of each particular system. In our case, the following assumptions[27,28] were made: (i) the diffusion process can be described by Fick's laws; (ii) the diffusion coefficient is constant during the desorption process (i.e., concentration-independent), which can be assumed when the concentration of solute is low; (iii) mass transfer only occurs in the direction of the film thickness (unidimensional diffusion), and edge effects are negligible; (iv) the only resistance to mass transfer is located in the polymer side (perfect sink conditions can be assumed in the air side); (v) the initial concentration of ketones in the film is uniform.

Moreover, due to the low concentration of ketones in the films, it was assumed that their diffusion rates are independent from each other. Therefore, the mathematical description of the ternary diffusion was simplified to a case of two pseudobinary diffusion processes.[29]

In this work, we applied the analytical solution of the second Fick's law proposed by Crank[27] for diffusion in thin slabs when the previous conditions (i–v) are assumed, in which the cumulative mass of solute released as a function of time is given by eq. (3)

$$\frac{M_t}{M_\infty} = 1 - \frac{8}{\pi^2}\sum_{n=0}^{\infty}\frac{1}{(2n+1)^2}\exp\left[-\frac{(2n+1)^2\pi^2}{L^2}Dt\right] \quad (3)$$

where M_t is the mass released after time t, M_∞ is the total released mass (or the initial ketone content in the film), L is the film thickness, and D is the diffusion coefficient of the solute in the film, considered concentration-independent. M_t and M_∞ for each ketone were calculated from gravimetric measurements and FTIR analysis, as previously explained. A schematic description of our system is represented in Figure 2.

Equation (3) has been previously applied by other authors for the mathematical description of desorption processes from polymers, both in gas and liquid phase, when the internal diffusion is the limiting step and provided the validity of the above mentioned assumptions. Some examples include the absorption of flavor compounds, such as terpenes, esters, and phenolics, by polymeric packaging films in fruit juices, wines, etc.[21,22,30–32] and the emission of volatile organic compounds (VOCs) (phenol, dodecane) from polymeric building materials.[33]

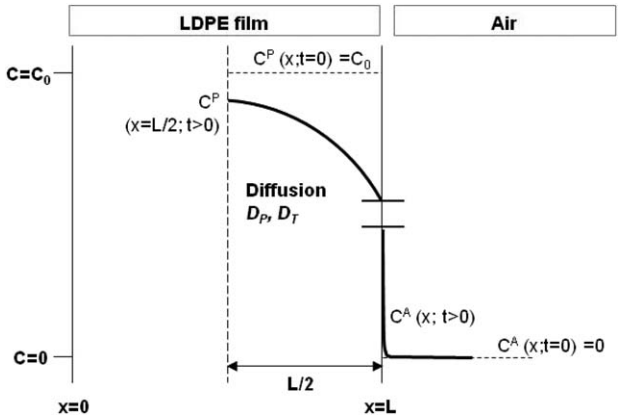

Figure 2. Schematic diagram of the ketone release process from a polymeric slab of thickness L to air: concentration profiles and equilibrium conditions in the LDPE/air interphase.

As can be seen, eq. (3) involves an infinite series of terms. In our calculations, only the first 20 terms were included, due to the fact that the contribution of the terms for $n > 20$ proved to be negligible. The model fitting was performed using the Microsoft Excel Solver tool, with D as adjustable parameter, and minimizing the sum of squared errors (SSE), calculated according to eq. (4)

$$\mathrm{SSE} = \sum_{i=1}^{\mathrm{NP}} \left[\left(\frac{M_t}{M_\infty} \right)_{\mathrm{exp}} - \left(\frac{M_t}{M_\infty} \right)_{\mathrm{calc}} \right]^2 \quad (4)$$

where NP is the number of experimental and calculated points.

The experimental procedure as well as the model suitability to reproduce experimental diffusion coefficient values was validated using LDPE films impregnated with eugenol, comparing the estimated diffusion coefficient for this compound in LDPE films with those reported by other authors. Eugenol was selected due to its chemical structure, molecular weight, and volatility behavior, which are closely related to the ketones studied in this work. The $scCO_2$-assisted impregnation process and conditions have been described in a previous work.[34]

Statistical Analysis. Two impregnated films were used for each release experiment, obtained under the same operational conditions, and were considered as replicas in the statistical analysis. The effect of each factor (pressure, depressurization rate, contact time, and initial ketone concentration in the fluid phase) and all two-factor interactions on the adjusted diffusion coefficient of each ketone in LDPE were statistically determined by analysis of variance (ANOVA) using the software Statgraphics (StatPoint Technologies, Inc. Warrenton, VA, US).[35] The effects of the factors were considered significant for $P < 0.05$ (95% confidence level).

RESULTS AND DISCUSSION

As previously mentioned, the validity of the experimental procedure and the mathematical approach was first verified by comparison with diffusion coefficient values of eugenol in LDPE reported in the literature. For that purpose, cumulative release curves were constructed using films impregnated with eugenol by $scCO_2$-assisted impregnation under different pressure (12 and 15 MPa) and depressurization rate (0.5 and 1.0 MPa min^{-1}) conditions.[34] The release experiments were performed at similar laboratory conditions as described in the Experimental section for the ketone-loaded films. The diffusion coefficient values obtained using eq. (3) were in the range of 2.0–4.5 $\times$ 10^{-14} m^2 s^{-1}, as shown in Figure 3. ANOVA testing of these results suggested that pressure and depressurization rate, as well as their interaction have significant effect on the diffusion coefficient of eugenol (D_E) in LDPE films, at tested conditions ($P < 0.05$). The range of values obtained for D_E are in good agreement with the results by Dhoot *et al.*[36] who have reported D values for eugenol in LDPE films in the range of 2.3–10.3 $\times$ 10^{-14} m^2 s^{-1}, determined both by attenuated total reflection-FTIR spectrometry and High performance liquid chromatography (HPLC), at 23 °C. Other authors have informed a somewhat higher value of 2.6 $\times$ 10^{-13} m^2 s^{-1} (also in LDPE, at 23 °C),[37] but information about the experimental conditions and procedure is not available in open literature to the best of our knowledge. Caution has to be taken when comparing experimental data obtained using different LDPE samples, as polymer density and morphology differences can introduce important variability in the observed results.

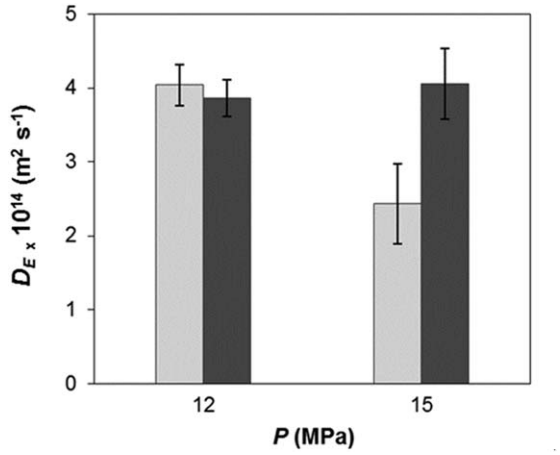

Figure 3. Diffusion coefficient (D_E) values for eugenol in $scCO_2$ impregnated LDPE films as a function of impregnation pressure and depressurization rate conditions: (■) 0.5 MPa min^{-1}, (■) 1.0 MPa min^{-1}. Vertical bars indicate standard deviation ($n = 3$).

In the case of thymoquinone and pulegone, Figure 4 shows an example of their cumulative release profiles corresponding to the samples impregnated at $P = 10$ and 15 MPa, with depressurization rate = 2 MPa min^{-1}, $T = 45$ °C, $t = 2$ h, and initial ketone mole fraction = 0.0017 (identified as runs 3 and 10 in Table I, respectively), as well as the corresponding adjusted model. As previously mentioned, FTIR analysis was performed in order to determine the release kinetics of each individual ketone in combination with the gravimetric method. For that purpose, characteristic absorption bands were identified and taken as reference for each compound: 1238 cm^{-1} for thymoquinone (assigned to C═C bonds) and 1208 cm^{-1} for pulegone (assigned to C—H bonds in the >CH—CH_3 group).[16] Figure 5 shows the characteristic bands of both ketones (after baseline correction and normalization using the band at 725 cm^{-1} as reference for polyethylene) and their evolution during the release process for a selected sample, corresponding to run 1.

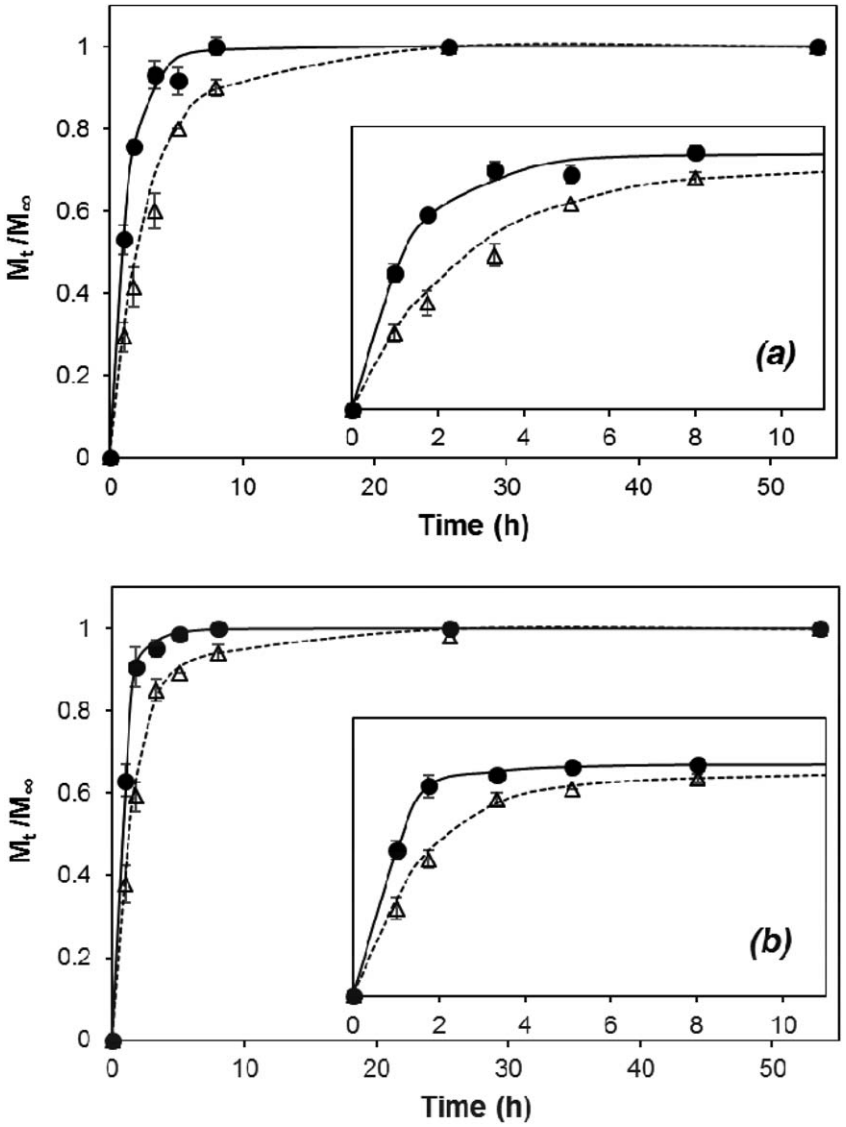

Figure 4. Release profiles of *R*-(+)-pulegone (a) and thymoquinone (b) in LDPE films impregnated at $P = 10$ MPa (△) and 15 MPa (●), with depressurization rate = 2 MPa min^{-1}, $T = 45\,°C$, $t = 2$ h, and initial ketone mole fraction = 0.0017. Dots: experimental data; lines: model fitting for $P = 10$ MPa (–-) and 15 MPa (---). Vertical bars indicate standard deviation ($n = 2$).

It can be seen in Figure 4 that the model is able to describe satisfactorily the observed release profiles under the assumption of Fickian behavior with a constant diffusion coefficient for each compound. It can also be noticed that thymoquinone is released at a faster rate than pulegone: while the first compound is practically exhausted within the first 10 h of exposure, the time required for pulegone is about 20 h. This trend was observed in all runs and it is reflected in higher estimated diffusion coefficient values for thymoquinone (D_T) than for pulegone (D_P), as shown in Table I for the complete experimental design. These values ranged from 2.35×10^{-13} to 5.53×10^{-13} m^2 s^{-1} for thymoquinone, and from 1.24×10^{-13} to 4.52×10^{-13} m^2 s^{-1} for pulegone, being D_T values between 20% and 100% higher than D_P values, depending on the impregnation conditions. In general, these values are comparable in order of magnitude to the diffusion coefficients reported in the literature for other similar terpenes in semi-crystalline LDPE at the same temperature, such as limonene (2–20 $\times 10^{-13}$ m^2 s^{-1}, at 22 °C),[32] pinene (9.7×10^{-13} m^2 s^{-1}, at 22 °C),[31] citral (3.5–5.5 $\times 10^{-13}$ m^2 s^{-1}, at 23 °C),[38] menthol (1.2×10^{-13} m^2 s^{-1}, at 23 °C),[37] and 1,8-cineol (1.0×10^{-13} m^2 s^{-1}, at 23 °C),[37] among others. As previously mentioned, direct comparison between different sets of data is difficult when the polymer properties vary, and therefore results should not be compared beyond the order of magnitude.

It is well known that the diffusion coefficient of a solute in a polymeric matrix depend on several factors, namely: solute properties, such as molecular weight and geometry (linear, cyclic, branched structure); polymer properties (chemical structure, polydispersity, density, crystallinity, crosslinking degree, etc.); the interactions between solute and polymer molecules; and ambient conditions, mainly temperature.[39] Considering that polyolefins (like LDPE) do not have functional groups capable of strong interactions with solute molecules, and that the release

Table I. Experimental Design of Impregnation Conditions and Estimated Diffusion Coefficients for Pulegone (D_P) and Thymoquinone (D_T)

Run no.	Pressure (MPa)	Depressurization rate (MPa min^{-1})	Time (h)	Initial ketone mole fraction	$D_P \times 10^{13}$ (m^2 s^{-1})	$D_T \times 10^{13}$ (m^2 s^{-1})
1	10	0.5	2	0.0017	1.24 ± 0.01	2.35 ± 0.13
2	10	0.5	2	0.0025	1.75 ± 0.07	2.81 ± 0.19
3	10	2.0	4	0.0017	1.77 ± 0.18	2.55 ± 0.41
4	10	2.0	4	0.0025	1.54 ± 0.16	3.03 ± 0.12
5	15	0.5	4	0.0017	3.09 ± 0.18	3.98 ± 0.05
6	15	0.5	4	0.0025	3.47 ± 0.07	4.22 ± 0.39
7	15	2.0	2	0.0017	3.00 ± 0.08	3.83 ± 0.28
8	15	2.0	2	0.0025	2.78 ± 0.05	3.84 ± 0.30
9	10	0.5	4	0.0017	2.09 ± 0.11	3.20 ± 0.15
10	15	2.0	4	0.0017	2.78 ± 0.18	3.50 ± 0.16
11	15	0.5	2	0.0025	4.52 ± 0.38	5.53 ± 0.84
12	10	2.0	2	0.0025	2.24 ± 0.52	3.50 ± 0.17

Mean values ± standard deviation with $n = 2$.
All impregnation runs were performed at $T = 45$ °C.

experiments were performed under controlled and constant ambient conditions, the differences observed between the diffusion coefficient of thymoquinone and pulegone in all samples under the same release conditions may be explained in terms of their own physicochemical properties. Regarding the molecular weight, thymoquinone is heavier than pulegone (164.2 vs. 152.2 g mol^{-1}), which should be reflected in a lower D value, in contrast with the observed behavior. However, a closer inspection to their geometric structure and spatial configuration indicates that thymoquinone is a planar molecule (due to the C=C bonds in the ring), while pulegone, which has a saturated cyclohexane ring, adopts preferentially a half-chair conformation.[40] This conformation probably has a higher steric hindrance than the planar one, sliding with more difficulty among polymer chains, and thus explaining the lower diffusion coefficient. A comparison of the D values of benzene (planar structure) and cyclohexane (chair conformation) in LDPE supports this hypothesis. In fact, several authors have reported comparative data for both compounds (measured in the same polymer) that indicate a higher diffusivity of benzene over cyclohexane: 9.9×10^{-13} versus 4.1×10^{-13} m^2 s^{-1} [41]; 2.15×10^{-12} versus 1.04×10^{-12} m^2 s^{-1} [42]; 3.8×10^{-13} versus 2.0×10^{-13} m^2 s^{-1} [43]; 2.0×10^{-12} versus 6.1×10^{-13} m^2 s^{-1},[44] all data measured at 23 °C. Besides, pulegone has a higher affinity for LDPE, as it has only one carbonyl group, which can also contribute to a higher retention in the polymer matrix.

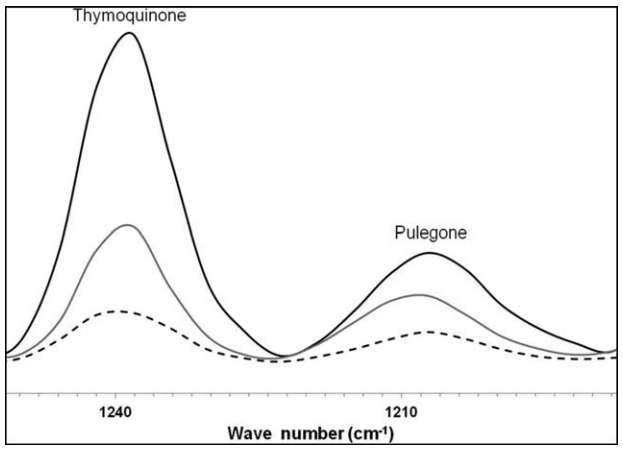

Figure 5. Progress along time of characteristic absorbance bands of thymoquinone and *R*-(+)-pulegone on FTIR spectra of ketone-loaded LDPE film (impregnated at $T = 45$ °C, $P = 10$ MPa, depressurization rate = 0.5 MPa min^{-1}, $t = 2$ h, and initial ketone mole fraction = 0.0017). Different spectra correspond to different release times: (—) $t = 0$ h; (—) $t = 1$ h; (- -) $t = 2$ h.

Results reported in Table I were statistically analyzed using ANOVA in order to determine the effect of each process variable and all binary interactions, as well as their significance. The results of this analysis are presented in Tables II and III for D_P and D_T, respectively. As mentioned before, effects were considered significant for P-values lower than 0.05. Results indicate that impregnation pressure, depressurization rate, and their combination are the only factors with significant effects on the observed differences in the diffusion coefficient values. The Pareto diagrams shown in Figure 6 represent graphically the standardized effect of each factor. As can be seen, impregnation pressure has a strong positive effect on the diffusion coefficient of both ketones in the loaded LDPE films. This enhancement of mass transfer properties with pressure can be related to the morphological changes that the polymer undergoes during the impregnation process.

In a typical $scCO_2$-assisted impregnation run in batch mode, the polymer is exposed to a three-step process: pressurization (generally slow), soaking at constant pressure for a certain time, and depressurization (fast or slow).[45] Under high pressure conditions, $scCO_2$ is sorbed by the polymer to a maximum extent determined by the thermodynamic solubility, which in turn depends on the pressure and temperature conditions, the possible interactions between CO_2 and polymer molecules, and the

Table II. ANOVA Testing the Effects of Process Variables on the Diffusion Coefficient of Pulegone (D_P) for the Fractional Design Model

Factor	DF	Effect	SS	MS	*F*	*P* value
A: Pressure	1.00	1.34	7.14	7.14	59.30	*<0.0001*
B: Depressurization rate	1.00	−0.47	0.90	0.90	7.45	*0.017*
C: Time	1.00	−0.28	0.31	0.31	2.60	0.131
D: Initial ketone mole fraction	1.00	0.11	0.05	0.05	0.39	0.542
AB	1.00	−0.55	1.23	1.23	10.18	*0.007*
AC	1.00	−0.36	0.50	0.50	4.19	0.062
AD	1.00	−0.03	0.00	0.00	0.03	0.860
BC	1.00	−0.18	0.13	0.13	1.05	0.325
BD	1.00	−0.33	0.45	0.45	3.70	0.077
CD	1.00	−0.32	0.54	0.54	4.45	0.055
Residual	13.00		1.57	0.12		

DF: degrees of freedom. SS: sum of squares. MS: mean square.

polymer morphology (amorphous or crystalline, glassy or rubbery).[9–13] CO_2 sorption induces two other related phenomena: the swelling of the matrix (i.e., an increase of its volume) and a certain plasticization degree, which are explained in terms of an increase of the system-free volume and the mobility of the polymer chains.[1] These changes enhance the diffusion of solute molecules into the polymer, which is the basis for the impregnation process. After some time of exposure under constant conditions (during which equilibrium can be attained or not), the system is depressurized by releasing the CO_2 (along with the remaining solute) at a given rate. Depending on the depressurization conditions, the polymer can recover (more or less partially) its original morphology or undergo irreversible modifications, such as foaming due to a very rapid CO_2 release.[15]

In a previous work concerning the $scCO_2$ impregnation of LDPE films (similar to the films used in this work) with eugenol, it was observed that the crystallinity degree of the polymer (determined by DSC) was reduced by the treatment, from an original value of 44.3% to 37.1–37.9% after impregnation.[34] This effect was not only due to the incorporation of eugenol: in fact, it was also observed in films exposed to $scCO_2$ under the same conditions but in the absence of this solute. The same phenomenon has been reported by other authors. Torres *et al.*[46] observed a decrease of crystallinity in linear LDPE films from 33.9% to 25.1–30.6% when treated with $scCO_2$ (at 45 °C and 7–12 MPa) in the presence or absence of thymol; and Rojas *et al.*[47] reported a decrease from 40% up to 25.8% in the case of impregnation (and simple pressurization) of linear LDPE films with 2-nonanone at 40 °C and different pressure (12–22 MPa) and depressurization rate conditions (1–10 MPa min^{-1}). In the last case, the crystallinity reduction increased with pressure and decreased with depressurization rate.

Crystallinity degree plays an important role in the diffusion of solutes in semicrystalline polymers. The classical picture of this kind of polymers consists in highly ordered crystalline domains (crystallites) embedded in an amorphous matrix. In the case of LDPE (with a glass transition temperature of ~–100 °C), the amorphous part is in the rubbery state. It is generally considered that solute molecules only dissolve and diffuse in the amorphous parts, being the crystallites practically impermeable

Table III. ANOVA Testing the Effects of Process Variables on the Diffusion Coefficient of Thymoquinone (D_T) for the Fractional Design Model

Factor	DF	Effect	SS	MS	*F*	*P* value
A: Pressure	1.00	1.20	5.76	5.76	25.14	*<0.0005*
B: Depressurization rate	1.00	−0.53	1.12	1.12	4.9	*0.045*
C: Time	1.00	−0.31	0.39	0.39	1.72	0.213
D: Initial ketone mole fraction	1.00	0.30	0.36	0.36	1.56	0.234
AB	1.00	−0.55	1.21	1.21	5.28	*0.039*
AC	1.00	−0.51	1.03	1.03	4.47	0.054
AD	1.00	−0.17	0.12	0.12	0.53	0.481
BC	1.00	−0.08	0.03	0.03	0.12	0.732
BD	1.00	−0.05	0.01	0.01	0.05	0.834
CD	1.00	−0.26	0.35	0.35	1.54	0.236
Residual	13.00	1.20	2.98	0.23		

DF: degrees of freedom. SS: sum of squares. MS: mean square.

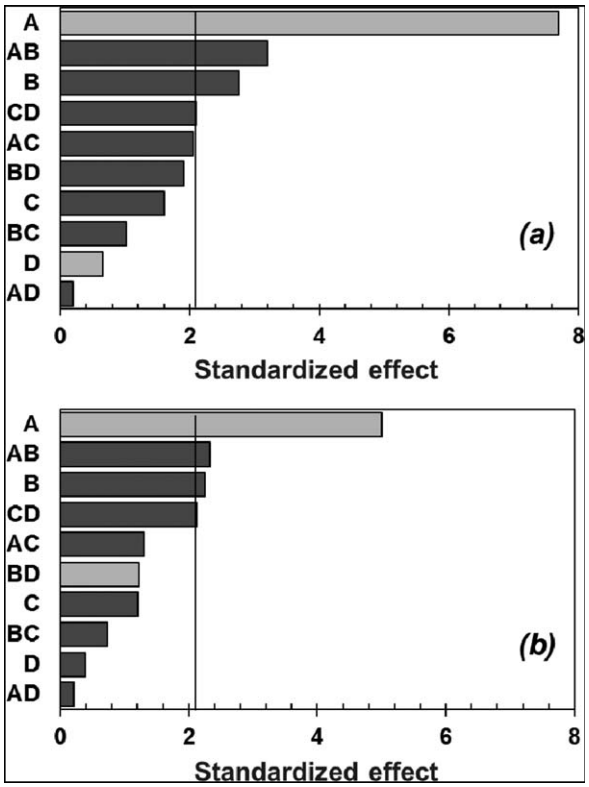

Figure 6. Pareto diagram for diffusion coefficient of *R*-(+)-pulegone (a) and thymoquinone (b) in $scCO_2$ impregnated LDPE films. A: pressure; B: depressurization rate; C: contact time; D: initial ketone mole fraction. Double letters represent binary factor interactions.

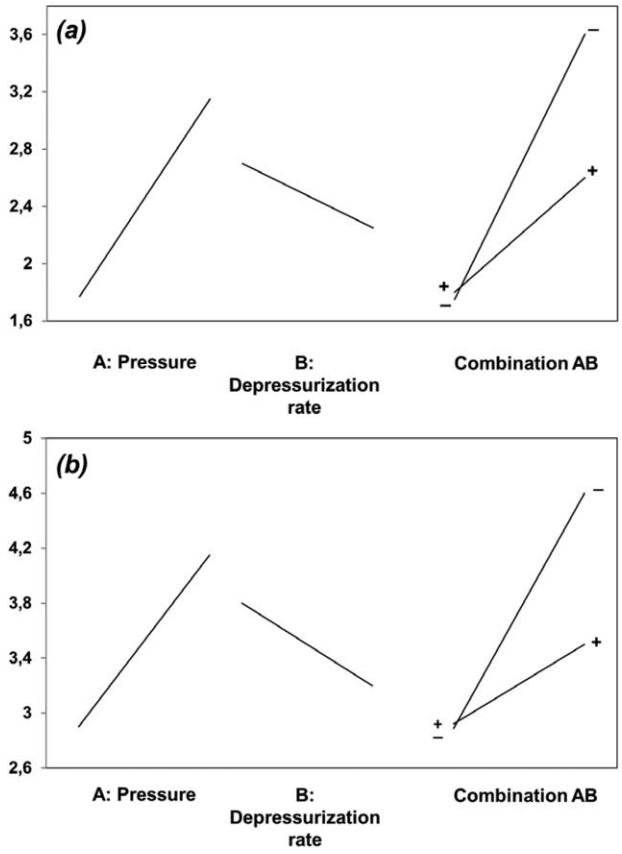

Figure 7. Single and interaction effects of pressure and depressurization rate on the diffusion coefficients of *R*-(+)-pulegone (a) and thymoquinone (b).

to diffusion.[48,49] Diffusion is therefore regarded as a tortuous motion of solute molecules through the amorphous region with the crystallites acting as "obstacles" to be surrounded.[39] Thus, an increase of crystallinity may reduce the observed diffusion coefficients by increasing the tortuosity, and inversely a decrease of crystallinity may enhance internal mass transfer. In this way, when the LDPE films are impregnated at a higher pressure (15 MPa), the crystallinity degree reduction of the material is higher, and therefore higher diffusion coefficients in the impregnated films are observed.

Regarding depressurization rate, the statistical analysis indicates that this factor has a negative effect on the diffusion coefficient of both ketones, as can be seen in Figure 6 and Tables II and III. In other words, a faster depressurization induces lower diffusion coefficient values. This is in agreement with the behavior reported by Rojas *et al.*[47] who observed a decrease of the diffusion coefficient values of 2-nonanone in impregnated linear LDPE films from 6.8×10^{-12} m^2 s^{-1} (in films depressurized at 1 MPa min^{-1}) to 3.0×10^{-12} m^2 s^{-1} (at 10 MPa min^{-1}). They ascribe this behavior to the mechanisms of incorporation of solute into the polymer, which would favor stronger interactions between them (or a higher cohesive energy) when the films are depressurized fastly. The explanation can also be related to the crystallinity degree reduction, as in the case of the effects of impregnation pressure. In fact, according to their data, the crystallinity decrease was smaller in the films depressurized at higher rate. In our case, the narrow range of depressurization rates studied (0.5 and 2 MPa min^{-1}) can account for the limited effect observed.

Concerning the interaction between impregnation pressure and depressurization rate, the effects on the diffusion coefficient values can be seen graphically in Figure 7. In addition, response surface plots for the effect of these two variables on the diffusion coefficients of *R*-(+)-pulegone and thymoquinone are shown in Figure 8. According to the statistical analysis, the depressurization rate practically has no effect on D_T and D_P when the impregnation is performed at 10 MPa (lower level), while it shows the already discussed negative effect when operating at 15 MPa (higher level). An explanation of this difference can be attempted again in terms of the effect of CO_2 sorption on the polymer morphology. As previously discussed, sorption is higher at 15 MPa, and therefore LDPE will be more plasticized. A faster depressurization could favor the polymer recrystallization induced by a rapid CO_2 desorption (and perhaps by a stronger local cooling effect due to pressure drop), effects that are less marked when depressurizing from 10 MPa.

Finally, according to the statistical analysis, impregnation time and initial ketone mass fraction in the $scCO_2$ phase have no significant effect on the diffusional properties of the impregnated films. It does not mean that these parameters have no real influence on the physicochemical processes that occur during

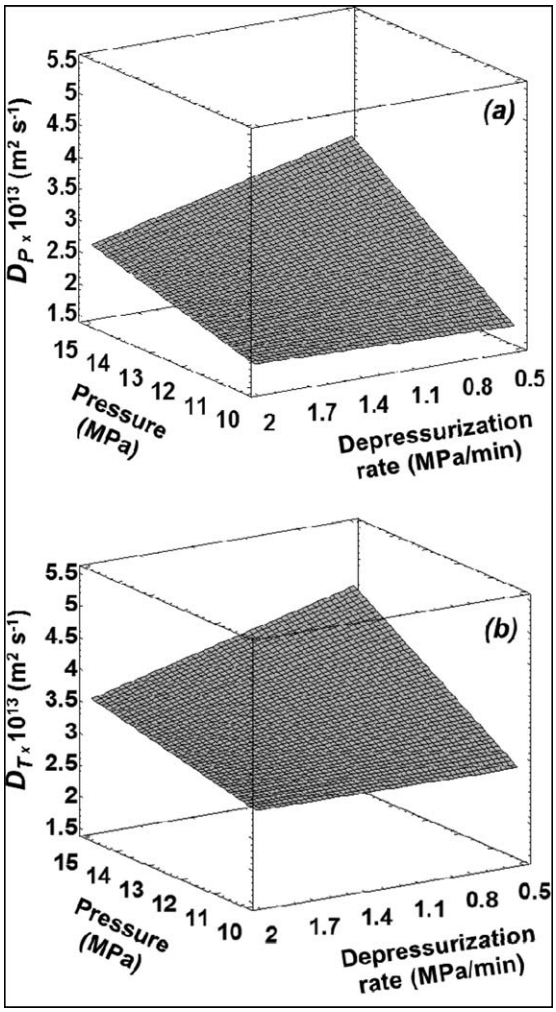

Figure 8. Response surface plots for the effect of pressure and depressurization rate on the diffusion coefficients of *R*-(+)-pulegone (a, D_P) and thymoquinone (b, D_T).

impregnation. In fact, as CO_2 sorption, polymer swelling, plasticization, and solute penetration are time-dependent process, the extent in which they occur will be determined by the duration of the impregnation process (until equilibrium is reached), with effects on the associated observed properties (crystallinity, diffusivity, solute loading, etc.).[50] The concentration of the fluid phase, which is the driving force for solute mass transfer to the polymer, also affects the solute loading, which in turn modifies the polymer morphology by plasticization. A deeper discussion of the effect of these factors on the impregnation yield has been reported in a previous work.[16] The fact that no significant effects were observed on the ketones diffusion coefficients due to these factors is probably related to the values selected in our screening experimental design, which may be too close among them to produce an appreciable difference.

CONCLUSIONS

In conclusion, the diffusion coefficients of thymoquinone and *R*-(+)-pulegone in LDPE films obtained by $scCO_2$ impregnation have been estimated by desorption experiments into air. The combination of gravimetric measurements (for total release) and FTIR spectrometric analysis (for the individual ketones) proved to be a practical method for rapid and non-destructive assessment. The cumulative release curves could be satisfactorily modeled by assuming Fickian diffusion behavior, and a good fitting was achieved with a single parameter, i.e., the diffusion coefficient value for each ketone.

The screening design of experiments applied for the study, along with the statistical analysis of the results, allowed to identify the impregnation process variables which significantly affect the observed diffusion coefficients (within the studied range of conditions): the operation pressure and the depressurization rate. Based on these results, as well as previous data and results reported by other authors, the effect of these parameters on the polymer morphological properties (crystallinity degree) and the diffusional properties has been discussed.

The knowledge of the diffusion coefficient values of both ketones in LDPE, as well as the effect of impregnation conditions on these values, are a very useful tool for the design of controlled release materials. In first place, it provides some indications for adjusting the material diffusional properties by performing the $scCO_2$ impregnation process under suitable conditions. In this way, if the release rate of ketones is to be minimized, the film impregnation should be conducted at lower pressure; or, inversely, if it has to be enhanced, impregnation should be performed at higher pressure and slow depressurization rate. And secondly, it is an important data for more complex mass transfer models applicable to more realistic applications: for example, the release of ketones in a confined environment (such as a silo bag), where the polymer/air partition equilibrium may also have an influence on the mass transfer profiles; or the diffusion through multilayered film structures, with different diffusional properties in each layer.

ACKNOWLEDGMENTS

The authors gratefully acknowledge Consejo Nacional de Investigaciones Científicas y Técnicas (CONICET, Argentina), Universidad Nacional de Córdoba (UNC, Argentina. SECyT 2015 Project), and Agencia Nacional de Promoción Científica y Tecnológica (ANPCyT, Argentina. PICT Startup 2011–0726) for their financial support. N.A. Gañán, M.C. Strumia, and R.E. Martini are career members of CONICET. M.L. Goñi also acknowledges CONICET for her postdoctoral fellowship.

REFERENCES

1. Kazarian, S. G. *Polym. Sci.* **2000**, *42*, 78.
2. Kikic, I.; Vecchione, F. *Curr. Opin. Solid State Mater. Sci.* **2003**, *7*, 399.
3. Kiran, E. *J. Supercrit. Fluids* **2016**, *110*, 126.
4. Chen, Y.; Zhang, Q.; Han, Q.; Mi, Y.; Sun, S.; Feng, C.; Xiao, H.; Yu, P.; Yang, C. *J. Appl. Polym. Sci.* **2017**, *134*, DOI: 10.1002/app.44721.

5. Geiger, B. C.; Nelson, M. T.; Munj, H. R.; Tomasko, D. L.; Lannutti, J. J. *J. Appl. Polym. Sci.* **2015**, *132*, DOI: 10.1002/app.42571.
6. Cocero, M. J.; Martín, Á.; Mattea, F.; Varona, S. *J. Supercrit. Fluids* **2009**, *47*, 546.
7. Nalawade, S. P.; Picchioni, F.; Janssen, L. P. B. M.; Grijpma, D. W.; Feijen, J. *J. Appl. Polym. Sci.* **2008**, *109*, 3376.
8. Kikic, I. *J. Supercrit. Fluids* **2009**, *47*, 458.
9. Pantoula, M.; Panayiotou, C. *J. Supercrit. Fluids* **2006**, *37*, 254.
10. Pantoula, M.; von Schnitzler, J.; Eggers, R.; Panayiotou, C. *J. Supercrit. Fluids* **2007**, *39*, 426.
11. Shieh, Y.-T.; Su, J.-H.; Manivannan, G.; Lee, P. H. C.; Sawan, S. P.; Spall, W. D. *J. Appl. Polym. Sci.* **1996**, *59*, 695.
12. Shieh, Y.-T.; Su, J.-H.; Manivannan, G.; Lee, P. H. C.; Sawan, S. P.; Spall, W. D. *J. Appl. Polym. Sci.* **1996**, *59*, 707.
13. Wissinger, R. G.; Paulaitis, M. E. *J. Polym. Sci. Part B: Polym. Phys.* **1987**, *25*, 2497.
14. Alessi, P.; Cortesi, A.; Kikic, I.; Vecchione, F. *J. Appl. Polym. Sci.* **2003**, *88*, 2189.
15. Üzer, S.; Akman, U.; Hortaçsu, Ö. J. *Supercrit. Fluids* **2006**, *38*, 119.
16. Goñi, M. L.; Gañán, N. A.; Herrera, J. M.; Strumia, M. C.; Andreatta, A. E.; Martini, R. E. *J. Supercrit. Fluids* **2017**, *122*, 18.
17. Herrera, J. M.; Zunino, M. P.; Massuh, Y.; Pizzollito, R.; Dambolena, S.; Gañan, N. A.; Zygadlo, J. A. *AgriScientia* **2014**, *31*, 35.
18. Herrera, J. M.; Zunino, M. P.; Dambolena, J. S.; Pizzolitto, R. P.; Gañan, N. A.; Lucini, E. I.; Zygadlo, J. A. *Ind. Crops Prod.* **2015**, *70*, 435.
19. Herrera, J. M.; Goñi, M. L.; Gañán, N. A.; Zygadlo, J. A. *Crop Prot.* **2017**, *98*, 33.
20. Goñi, M. L.; Gañan, N. A.; Barbosa, S. E.; Strumia, M. C.; Martini, R. E. J. *Supercrit. Fluids, to appear.* DOI: 10.1016/j.supflu.2017.06.013.
21. Sadler, G. D.; Braddock, R. J. *J. Food Sci.* **1991**, *56*, 35.
22. Peychès-Bach, A.; Moutounet, M.; Peyron, S.; Chalier, P. *J. Food Eng.* **2009**, *95*, 45.
23. Sicardi, S.; Manna, L.; Banchero, M. *J. Supercrit. Fluids* **2000**, *17*, 187.
24. Petropoulos, J. H. In Polymeric Gas Separation Membranes; Paul, D. R., Yampol'skii, Y. P., Eds.; CRC Press, Inc.: Boca Raton, USA, **1994**; Chapter 02.
25. Theodorou, D. N. In Diffusion in Polymers; Neogi, P., Ed.; Marcel Dekker, Inc.: New York, **1996**; Chapter 02, p 67.
26. Haslam, J.; Willis, H. A.; Squirrell, D. C. M. Identification and Analysis of Plastics, 2nd ed.; Iliffe Books: London, **1972**.
27. Crank, J. The Mathematics of Diffusion; Oxford Univ. Press: London, **1975**; p 414.
28. Siepmann, J.; Siegel, R. A.; Siepmann, F. In Fundamentals and Applications of Controlled Release Drug Delivery; Siepmann, J., Siegel, R. A., Rathbone, M., Eds.; Springer: New York, **2012**; Chapter 06, p 127.
29. Cussler, E. L. In Multicomponent Diffusion; Churchill, S. W., Ed.; Elsevier Scientific Publishing Company: Amsterdam, **1976**, p 176.
30. Safa, L.; Abbes, B. *Packag. Technol. Sci.* **2002**, *15*, 55.
31. Cava, D.; Lagarón, J. M.; López-Rubio, A.; Catalá, R.; Gavara, R. *Polym. Test.* **2004**, *23*, 551.
32. Cava, D.; Catala, R.; Gavara, R.; Lagaron, J. M. *Polym. Test.* **2005**, *24*, 483.
33. Cox, S. S.; Zhao, D.; Little, J. C. *Atmos. Environ.* **2001**, *35*, 3823.
34. Goñi, M. L.; Gañán, N. A.; Strumia, M. C.; Martini, R. E. *J. Supercrit. Fluids* **2016**, *111*, 28.
35. Montgomery, D. C. Design and Analysis of Experiments, 8th ed.; Wiley: Hoboken, NJ, USA, **2013**.
36. Dhoot, G.; Auras, R.; Rubino, M.; Dolan, K.; Soto-Valdez, H. *Polymer (Guildf).* **2009**, *50*, 1470.
37. Koszinowski, J.; Piringer, O. *Beilage* **1990**, *41*, 15.
38. Lagarón, J. M.; Cava, D.; Giménez, E.; Hernandez-Muñoz, P.; Catala, R.; Gavara, R. *Macromol. Symp.* **2004**, *205*, 225.
39. Schlotter, N. E.; Furlan, P. Y. *Polymer* **1992**, *33*, 3323.(Guildf).
40. Suga, T.; Imamura, K. *Bull. Chem. Soc. Jpn.* **1972**, *45*, 2060.
41. McCall, D. W.; Slichter, W. P. *J. Am. Chem. Soc.* **1958**, *80*, 1861.
42. Takeuchi, Y.; Okamura, H. *J. Chem. Eng. Jpn.* **1976**, *9*, 136.
43. Fleischer, G. *Polym. Commun.* **1985**, *26*, 20.
44. Saleem, M.; Asfour, A.-F. A.; De Kee, D. *J. Appl. Polym. Sci.* **1989**, *37*, 617.
45. Champeau, M.; Thomassin, J.-M.; Tassaing, T.; Jérôme, C. *J. Control. Release* **2015**, *209*, 248.
46. Torres, A.; Romero, J.; Macan, A.; Guarda, A.; Galotto, M. J. *J. Supercrit. Fluids* **2014**, *85*, 41.
47. Rojas, A.; Cerro, D.; Torres, A.; Galotto, M. J.; Guarda, A.; Romero, J. *Fluids* **2015**, *104*, 76.
48. Hedenqvist, M. *Prog. Polym. Sci.* **1996**, *21*, 299.
49. Hedenqvist, M.; Angelstok, A.; Edsberg, L.; Larssont, P. T.; Gedde, U. W. *Polymer (Guildf).* **1996**, *37*, 2887.
50. von Schnitzler, J.; Eggers, R. *J. Supercrit. Fluids* **1999**, *16*, 81.